Title

Transcriptional drift in aging cells: A global decontroller.

Journal

Proceedings of the National Academy of Sciences, 121(30)

Authors

Matsuzaki, Tyler
Weistuch, Corey
de Graff, Adam
et al.

Publication Date

2024-07-23

DOI

10.1073/pnas.2401830121

Peer reviewed

PNAS RESEARCH ARTICLE | SYSTEMS BIOLOGY
BIOPHYSICS AND COMPUTATIONAL BIOLOGY

Transcriptional drift in aging cells: A global decontroller

Tyler Matsuzaki[a,1], Corey Weistuch[b,1], Adam de Graff[c], Ken A. Dill[a,2], and Gábor Balázsi[a,d,e,2]

Contributed by Ken A. Dill; received January 26, 2024; accepted June 11, 2024; reviewed by Murat Acar and Jean Hausser

As cells age, they undergo a remarkable global change: In transcriptional drift, hundreds of genes become overexpressed while hundreds of others become underexpressed. Using archetype modeling and Gene Ontology analysis on data from aging *Caenorhabditis elegans* worms, we find that the up-regulated genes code for sensory proteins upstream of stress responses and down-regulated genes are growth- and metabolism-related. We observe similar trends within human fibroblasts, suggesting that this process is conserved in higher organisms. We propose a simple mechanistic model for how such global coordination of multiprotein expression levels may be achieved by the binding of a single factor that concentrates with age in *C. elegans*. A key implication is that a cell's own responses are part of its aging process, so unlike wear-and-tear processes, intervention might be able to modulate these effects.

aging | transcriptional drift | archetype analysis

Significance

Our current inability to effectively decelerate human aging motivates our research into transcriptional drift—a global change in the expression of hundreds of genes across the lifespan. Here, we quantitate transcriptional drift in the model organism *Caenorhabditis elegans* and suggest that it is caused by linear changes in a single global regulatory factor. Given the conservation of this aging phenotype within human fibroblasts, our findings identify a system-wide biomarker with the potential to improve antiaging drug screening.

Upon aging, cells can undergo changes that are either *extrinsic* to the cell (nonautonomous), including signaling between tissues, or *intrinsic* to the cell (autonomous). Cell-intrinsic factors can be roughly classified into two types: either 1) *wear-and-tear*, or 2) *the cell's responses*, i.e., adaptive actions taken by the cell in response to aging. Examples of wear-and-tear include when mitochondria become less effective (1, 2), membranes become leaky (3–5), DNA, lipids, and proteins accumulate damage (6–8), and protection within the proteostasis system weakens (9–11).

A manifestation of aging is changes in gene expression. On the one hand, with some notable exceptions (12), aging can be associated with increases in transcriptional noise, which is the cell-to-cell variation in gene expression and which results in variations in mRNA and protein levels (13–15).

On the other hand, of interest here, Rangaraju et al. have recently explored more systematic changes in gene expression in aging *Caenorhabditis elegans* worms, which they call *transcriptional drift*. In transcriptional drift, hundreds of genes become increasingly overexpressed with age (relative to younger cells) while hundreds of others become increasingly underexpressed within the same cell (14). Transcriptional drift has been observed not only in adult *C. elegans*, where cells do not reproduce, but also within mice and humans (14, 16), organisms that age much slower than their constituent cells (17). In the latter, cell populations are constantly rejuvenated by the loss of old cells and the gain of new cells through division and differentiation. While similar large-scale concerted changes in gene expression occur in the Environmental Stress Response (ESR) (18) in yeast and the Integrated Stress Response (ISR) (19) in worms and higher organisms to combat stress, the ESR and ISR are typically only transient, whereas transcriptional drift is prolonged and persists over the full process of aging. Moreover, transcriptional drift is interesting because it may arise primarily as an actionable cell response to aging and thus potentially be susceptible to intervention. In support of this notion, inhibiting transcriptional drift extends the lifespan of *C. elegans* (14).

In the present work, we analyze the *C. elegans* transcriptomic time-course profile data from Rangaraju et al. (14). The experiment was conducted over 10 d which spans the organism's reproductive lifespan (8 d) and 67% of the typical lifespan (15 d) (20). First, using Normalized Nonnegative Matrix Factorization (N-NMF) to analyze patterns in the data in an unbiased way, we identify two underlying archetypes that capture this concerted transcriptional variation with age. Second, we use gene ontology (GO) analysis to determine which cell functions are involved in these archetypes, i.e., which functions are up- and down-regulated in aging. Third, we propose a simple biophysical model to explain how such many-protein coordination could be achieved in a simple way in response to aging. Finally, we validate our findings in human fibroblasts using transcriptomic data from Sturm et al. (21).

Author affiliations: [a]Louis and Beatrice Laufer Center for Physical and Quantitative Biology, Stony Brook University, New York, NY 11794; [b]Department of Medical Physics, Memorial Sloan Kettering Cancer Center, New York, NY 10065; [c]InVitro Cell Research, Englewood, NJ 07631; [d]Department of Biomedical Engineering, Stony Brook University, New York, NY 11794; and [e]Stony Brook Cancer Center, Stony Brook University, New York, NY 11794

Author contributions: C.W., K.A.D., and G.B. designed research; T.M. and C.W. performed research; C.W. contributed new reagents/analytic tools; T.M. and C.W. analyzed data; and T.M., C.W., A.d.G., K.A.D., and G.B. wrote the paper.

Reviewers: M.A., Koc Universitesi; and J.H., Karolinska Institutet Institutionen for cell- och molekylaabiologi.

The authors declare no competing interest.

[1]T.M. and C.W. contributed equally to this work.

[2]To whom correspondence may be addressed. Email: dill@laufercenter.org or gabor.balazsi@stonybrook.edu.

This article contains supporting information online at https://www.pnas.org/lookup/suppl/doi:10.1073/pnas.2401830121/-/DCSupplemental.

Published July 16, 2024.

Gene Grouping by Archetype Analysis

To verify the observed patterns in transcriptional drift, we applied Normalized Nonnegative Matrix Factorization to the data of Rangaraju et al. (14). This allowed us to identify concerted temporal gene expression signatures in the data. NMF is a widely used clustering algorithm for decomposing high-dimensional nonnegative signals into their dominant constituent parts (22). Somewhat like Principal Component Analysis, these component parts or *archetypes* represent coupled collections of signals that, roughly, behave the same way. However, this approach has two key advantages. First, the components tend to cluster the signals into distinct parts (22, 23). Second, by adding a normalization constraint, our N-NMF approach gives the relative contributions of the parts to each data sample. This method, which we detail in *SI Appendix*, has recently been used to identify and score the enrichment of distinct functional modules in many-gene cancer expression data (24, 25). Our treatment allows us to find patterns within the transcriptional data in an unbiased manner and evaluate how the components of these patterns evolve.

One principal finding is that the aging *C. elegans* data is best represented by two dominant *archetypes* (*SI Appendix*, Fig. S1). Each archetype is a grouping of hundreds of genes. An archetype can be thought of as an idealized exemplar, a kind of functional averaging over types of proteins, that best characterizes the behavior (increasing or decreasing with age) within the group (26). In our dataset, the archetypes that emerged were genes that had either monotonically increasing or monotonically decreasing expression levels measured in counts per million (cpm) over time, validating the observed patterns of Rangaraju et al. The relative contributions of these two archetypes to the total *C. elegans* gene expression varies over time (Fig. 1) and represents the concerted transcriptional changes associated with aging.

Although the patterns that emerged from N-NMF are not novel discoveries, our archetype analysis allowed us to quantitatively measure how well each gene follows the archetypes of the transcriptome. Fig. 2*A* shows a histogram of Pearson Correlations among gene expression levels in *C. elegans* between the increasing archetype and individual gene expression time-course data. The figure shows the number of genes for which expression tends to go down (*Left*) or up (*Right*), as a function of age. A remarkably large fraction of the whole genome changes systematically with age—either up or down—as seen by the areas under the curve of the two peaks on the *Left* and *Right*.

We leveraged this to extract and examine the concerted time-dependent behaviors of the most representative genes in the relative composition of the *C. elegans* archetypes. By examining these genes, we reasoned we would gain better insight into the driving forces behind the archetypes. We refer to these genes as our archetype centers, since they dominate the changes in proteome composition. We defined these archetype centers as genes that have a Pearson correlation coefficient with the global archetypes of ≤ -0.9 or ≥ 0.9, for a total of 1,859 down-regulated and 3,006 up-regulated genes, respectively. These dominant components are indicated to the *Left* and *Right* of the purple lines in Fig. 2*A*. The expression of these genes is plotted in Fig. 2*B*. From visual inspection, we noted that the up-regulated archetype centers tended to increase roughly linearly with age. In contrast, the down-regulated archetype centers tended to decrease nonlinearly, similar to a saturating function like a Michaelis–Menten binding process.

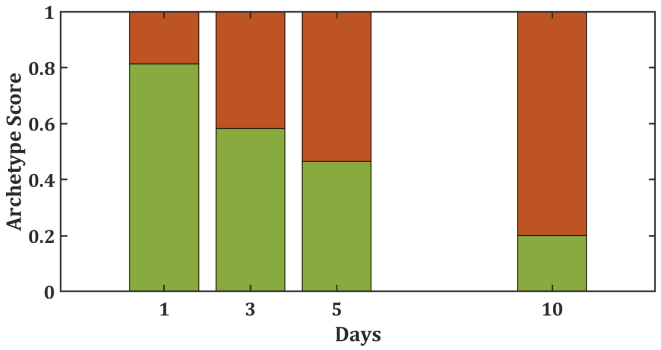

Fig. 1. The relative changes of the two archetypes of genes with age. Using normalized nonnegative matrix factorization, we identified two key archetypes: one that increases with age (red) and one that decreases (green).

GO Analysis of Protein Functions

To determine what biological functions are systematically up-regulated and down-regulated with age, we analyzed each archetype center using PANTHER GO Enrichment Analysis for functional classifications with Fisher's Exact Test (27–29). This allowed us to compare which genes were overrepresented in each subset compared to our reference list (consisting of all genes in the full dataset). Dataset S1 gives the results of our GO analysis, ordered by fold enrichment.

We found that the up-regulated archetype is enriched in functions related to sensing and transmitting signals (henceforth referred to as signaling genes). Genes having increased expression include acy-2, an adenylyl cyclase, and str-88, a G protein-coupled receptor (GPCR) protein, and genes involved in nervous system processes (116 genes), particularly those that act through G protein-coupled receptor activity (140 genes) and neurotransmitter receptor activity (36 genes). This heightened allocation to signaling *between* cells is in contrast to the downregulation we saw next of processes *within* cells.

We found the down-regulated archetype involves growth processes that run the day-to-day metabolic and protein turnover processes inside the cell (henceforth referred to as growth genes). Those having reduced expression include cullin-5, a ubiquitin protein ligase, and atp-2, the beta subunit of adenosine triphosphate (ATP) Synthase. More broadly, they include the pathways for mammalian target of rapamycin (mTOR) signaling, mRNA surveillance, and protein degradation (proteasome) that regulate growth, as well as glycolysis/gluconeogenesis, the tricarboxylic acid (TCA) cycle, and oxidative phosphorylation that power this growth. Also down-regulated are components of ATP Synthase, which is notable given its importance both in aging mice (30) and in the regulation of mTOR signaling and transcriptional drift (31).

Overall, *C. elegans*'s large-scale transcriptional drift appears to take a quasi-beneficial or adaptive path where synthesis of high-biomass pathways consisting of long-lived proteins are made early in life (thus down-regulated with age), while signaling processes needed to sense the environment and coordinate beneficial actions are relatively overexpressed later in life.

A Proposed Mechanism: The Cumulative Factor Model

What mechanism might explain such large-scale coordination of up-regulated and down-regulated protein levels with age? Here, we propose a minimalist model in which simply the

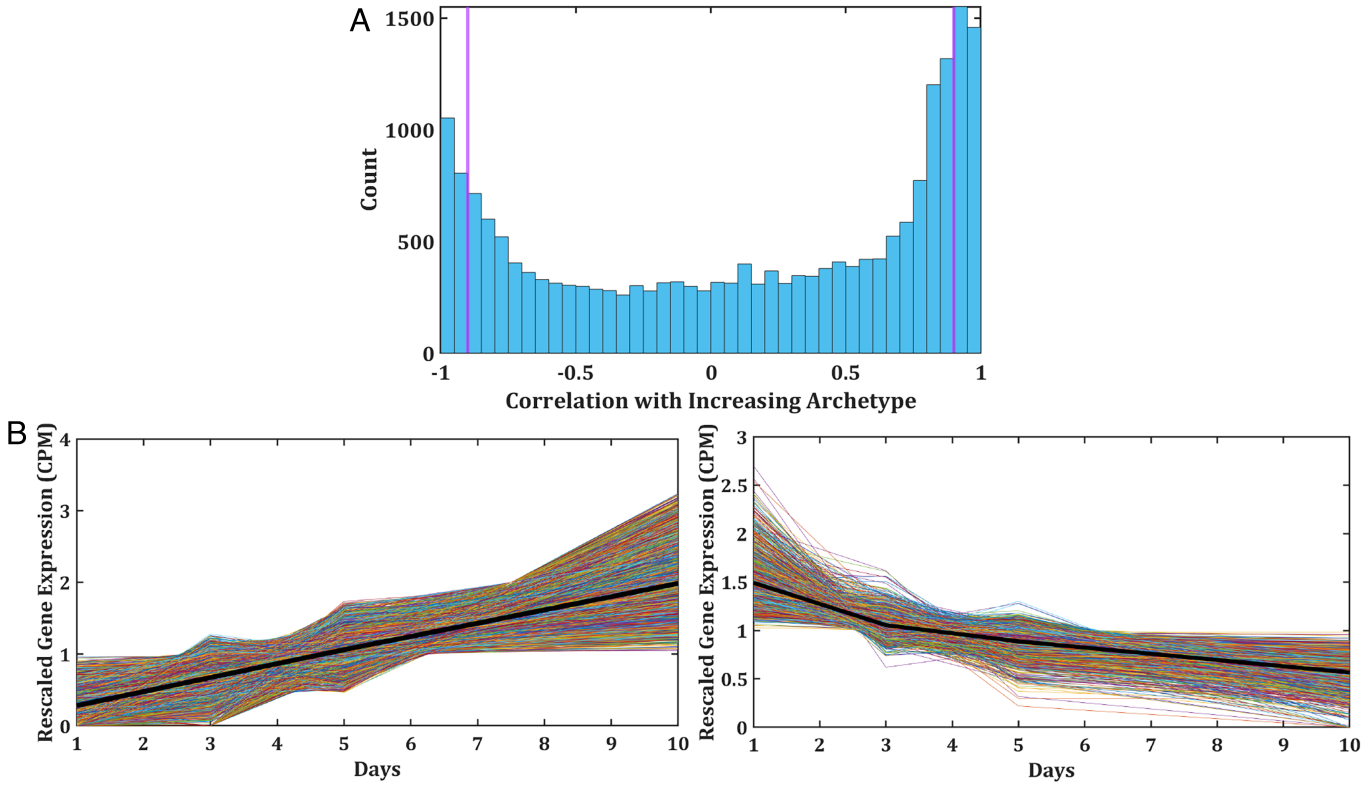

Fig. 2. Much of the transcriptome changes with age. (*A*) Pearson correlation coefficient of all genes with the increasing archetype. Genes with high positive R^2 are strongly monotonically increasing whereas genes with high negative R^2 are monotonically decreasing. Genes selected as archetype centers are to the *Left* and *Right* of the purple lines. (*B*) Rescaled expression data for genes with correlation coefficients ≥0.9 (*Top*) and ≤ −0.9 (*Bottom*). The black lines represent the mean trajectory to better illustrate the shape of the curves.

concentration $[f]$ of a single underlying molecular factor f—say, some ligand or protein—rises passively with age. This could result from some age-related decline, such as in proteostasis (32) or metabolism (2), or it could represent an age-related program that changes proteome composition and energy expenditure in a way that improves fitness (33, 34). Also, there is evidence for self-destructive processes in *C. elegans* (35). Regardless of the exact mechanism, a single such factor would be sufficient to drive concerted expression levels of large subsets of the genome (36).

Here's how it could work. Suppose the factor concentration $[f]$ accumulates linearly with age. If t is the cell's adult age (the time since completion of larval development), then the concentration of f at time t is

$$[f] = at, \qquad [1]$$

where a is a constant rate of accumulation of the factor.

Next, we describe how the cell turns that aging signal into a modulation of gene expression levels in the model. We suppose that sensory genes are precursors to genes that respond to stress (37). The cell uses these sensory or "signal" genes to detect the type of stress (start/end of starvation, oxidative, osmotic, DNA damaging stress, etc.), and signaling initiates cellular responses to counteract the stress as an attempt to reestablish homeostasis (38). Thus, we assume that signal genes correlate with stress genes.

In a young cell, we expect that the number of mRNAs and proteins involved in growth are in some optimal balance relative to those involved in signaling/stress. The data indicate that at time $t = 0$, in young cells, we have an initial level of signal genes s_0, averaged over all the corresponding proteins in that class. Similarly, the cell will also have an initial level of growth genes g_0. We suppose that $s_0 < g_0$ since a young cell has seen little stress yet and is poised to grow. However, cells will naturally experience stress throughout their day-to-day activities. This creates a gradual change in transcriptome regulation and proteotoxic stress which the cell must adapt to, resulting in a necessary increase in signal-related gene expression (14, 37).

The cell can detect its age by monitoring $[f]$ through Langmuir-type binding of f to a stress-sensor biomolecule. Thus, the number of signal mRNAs, s, will be

$$s = s_0 + \beta\left(\frac{[f]}{K_s + [f]}\right), \qquad [2]$$

$$\Longrightarrow \Delta s = s - s_0 \approx \left(\frac{\beta a}{K_s}\right) t = bt > 0. \qquad [3]$$

where s_0 is the initial concentration of the average signal mRNAs, K_s is a binding association constant, β gives the number of molecules binding and $b = \beta a/K_s$ is the slope of the time dependence in units of s per unit time. Mathematically, s_0 is the minimum value of s, at time zero and the signal gene expression is an increasing function of age. Because these time courses are observed to be linear, we can approximate $a \ll K_s$. So we can fit the experimental data with a single parameter b, which gives mechanistic insight because it is proportional to the average number of mRNA copies made for the signaling/stress subgenome.

The same mechanism applies to the growth genes:

$$\Delta g \;= g - g_0 \;= \frac{g_0 K_g}{K_g + [f]} - \gamma \;= \frac{g_0 K}{K + t} - g_0 < 0, \qquad [4]$$

Table 1. Parameter values for equation fits

Gene	Parameter	Value with 95% confidence bounds
Signal	b	$0.592 \pm 0.005\ d^{-1}$
Growth	γ	0.98 ± 0.40
Growth	K	3.3 ± 2.7 d

Here, g_0 is the maximum value of g, which occurs at the youngest age since g is a decreasing function of age. $K = K_g/a$ is the binding association constant for growth genes. Since the levels of the growth genes are not linear in age (unlike the signal genes), we now require two parameters, g_0 and K, to fit the experimental data. The necessity of this second parameter was validated using the Akaike information criterion (AIC) during model fitting.

Fitting to Experimental Data. We now use the experimental data to assess these linear and Michaelis–Menten binding mechanisms. Rangaraju et al. reported their data on transcriptional drift for each particular gene as $\mathrm{TD}_{\mathrm{ratio}} = \mathrm{cpm}_x/\mathrm{cpm}_0$, where cpm (counts per million reads mapped) refers to the expression level of a gene as measured through RNA-seq, and where the subscripts indicate day number $\times$ starting from day 0, which is the first day sexual maturity is reached (14). Our purposes here are best served by normalizing relative to day 0, $\mathrm{cpm}_x - \mathrm{cpm}_0$, to allow equal ranges between increasing and decreasing changes (since division restricts decreases to $[0, 1]$ and increases to $[1, \infty]$). We also scaled relative to the mean to prevent overemphasis on outliers, so instead we use

$$\mathrm{TD}_{\mathrm{diff}} = \frac{\mathrm{cpm}_x - \mathrm{cpm}_0}{\mathrm{cpm}_{\mathrm{mean}}}, \qquad [5]$$

where $\mathrm{cpm}_{\mathrm{mean}}$ is the mean cpm across the time points we analyzed. This allowed for better comparisons between genes without changing the overall shape of the data. Note that Δs measures TD_{diff} for signaling genes and Δg measures TD_{diff} for growth genes. In addition, the formula for $\mathrm{TD}_{\mathrm{diff}}$ is similar to the (rescaled) percent change in expression for an individual gene, $\mathrm{PC}_{\mathrm{exp}}$:

$$\mathrm{PC}_{\mathrm{exp}} = 100 * \frac{\mathrm{cpm}_x - \mathrm{cpm}_0}{\mathrm{cpm}_{\mathrm{mean}} * \mathrm{cpm}_0} = \frac{100}{\mathrm{cpm}_0} * TD_{\mathrm{diff}}. \qquad [6]$$

Thus, $\mathrm{PC}_{\mathrm{exp}}$ is a more interpretable measure of $\mathrm{TD}_{\mathrm{diff}}$, and by extension, Δs and Δg.

We used Eq. **3** to create best-fit curves to the average $\mathrm{PC}_{\mathrm{exp}}$ of archetype center genes in our signaling archetype. This allowed us to approximate a value for $[f]$ since it is directly correlated with b, the resulting best-fit coefficient. We then used this to fit Eq. **4** to the average $\mathrm{PC}_{\mathrm{exp}}$ of the growth archetype center genes using Eq. **4**. These best-fit parameters are listed in Table 1. As demonstrated in Fig. 3, both equations give good fits for the experimental $\mathrm{PC}_{\mathrm{exp}}$ with R^2 values of > 0.99. In addition, compared to linear models (AIC = 15.9), we found that Eq. **4** captured the data significantly better (AIC = 13.9), showing the need for a nonlinear model of the archetypes as a whole. We further validated that these results were due to individual gene behavior (and not an emergent property of the gene group) by fitting the cumulative factor model equations to the data of each individual gene (*SI Appendix*, Fig. S2). This supports that our model can predict the aging trajectories of our signaling and growth archetype centers. Taken together with the observation that drugs and longevity genes can broadly delay this drift (14), this supports the hypothesis that signaling and growth genes are coordinated—rising and falling together under shared control—because each group's behavior is characterized by their dependence on a shared variable, $[f] = at$.

Validation in Human Fibroblasts

To determine the generalizability of patterns in transcriptional drift to other organisms and cell types, we analyzed transcriptomics time course data within human fibroblasts from the data of Sturm et al. (21). In this study, human fibroblast samples collected from healthy humans were grown for 200 to 300 d, until the doubling time of the sample became larger than 30 d, which the authors argued represented the end of the cells' lifespan. We repeated our archetype analysis on this dataset and found a similar trend: The data were best represented by one monotonically increasing and one monotonically decreasing archetype, as seen in Fig. 4.

We then examined the archetype centers of the human fibroblast data in the same manner as *C. elegans* (Fig. 5). Although the downgoing genes followed a similar Michaelis–Menten type curve as in *C. elegans*, the upgoing genes appear to show a sigmoidal shape well-fit by a Hill function with a coefficient ≈2.8 (*SI Appendix*, Fig. S3). This difference is not surprising, considering that *C. elegans*, cells stop dividing at adulthood and age simultaneously by a self-destructive process (35), whereas human fibroblasts still divide in the dish as they do in the human body, where their cell population is also constantly rejuvenated by newly differentiating cells. The aging of single cells underlies the aging of whole organisms, but it occurs at a different organizational and temporal scale (17). Consequently, the reason for sigmoidal rather than linear upgoing trends might be differences in cell–cell interactions that mediate aging. Nonetheless, we still observe the essence of transcriptional drift

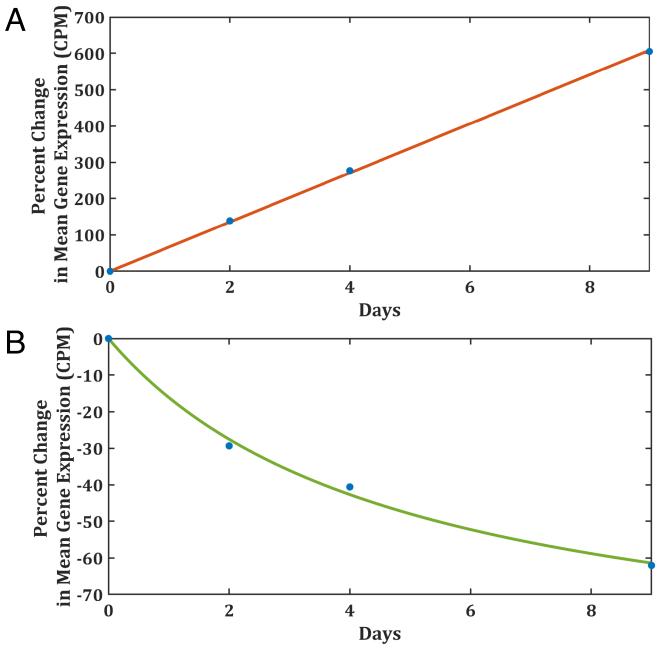

Fig. 3. The cumulative factor model captures the linear increase in up-regulated expressions and the Michaelis–Menten decrease in down-regulated expressions.. Best-fit regressions to the data using the equations in the text. The average value of $\mathrm{PC}_{\mathrm{exp}}$ across all genes in each subset is plotted in blue. (*A*) models the signaling genes with an R^2 of 0.9999 and (*B*) models the growth genes with an R^2 of 0.9964.

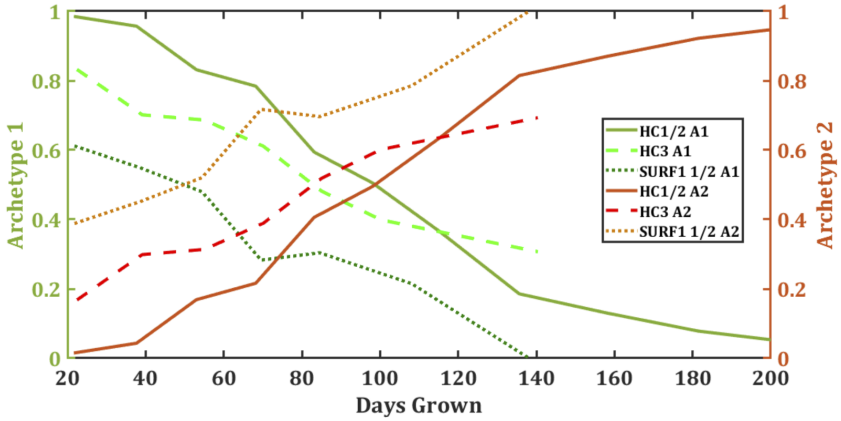

Fig. 4. Monotonically increasing and decreasing archetypes trajectories are present in human fibroblasts and can distinguish between increased aging mutations. HC cells are normal human fibroblasts, whereas SURF1 cells are fibroblasts with an accelerated aging mutation. A1 and A2 represent the two archetypes for each cell line. Our model was trained on technical replicates HC1 and HC2, then validated on technical replicate HC3 to show that similar cells show archetypes with similar trajectories. We then applied our model to SURF1 technical replicates 1 and 2 which produced archetypes that have lower/higher values at any given time point for the decreasing/increasing trajectories, suggesting that these cells have accelerated aging.

in human fibroblasts which is the focus of our paper. Indeed, we also saw similar patterns in the types of gene functions in the archetype center genes as *C. elegans*. Dataset S2 shows selected gene ontologies from both archetypes, indicating that signaling genes tended to be overexpressed and growth genes were underexpressed with age.

In addition, the authors collected data for fibroblasts containing the mitochondrial SURF1 mutation which causes hypermetabolism and accelerated biological aging (39). We reasoned that our pretrained model may be able to distinguish the accelerated aging phenotype. By examining the trajectory of the same representative genes, we found that the resulting archetypes in the SURF1 mutants were further along in the aging process compared to the normal fibroblast cells at any given timepoint (Fig. 4). Using this method, we believe that we can look for factors that accelerate or decelerate aging in future Perturb-seq experiments, helping to discern the identity of our model's factor f. In addition, this would provide valuable insight into discovering which drugs can extend lifespan.

Altogether, this suggests that transcriptional drift is a feature present not only in *C. elegans*, but also in fast-aging human cells that participate in the much slower process of human aging. Our findings are generalizable across the two species, with similar trajectories and gene functions changing with age. Last, we also show that we can use our archetype analysis method to distinguish between lifespan-extending and lifespan-shortening factors.

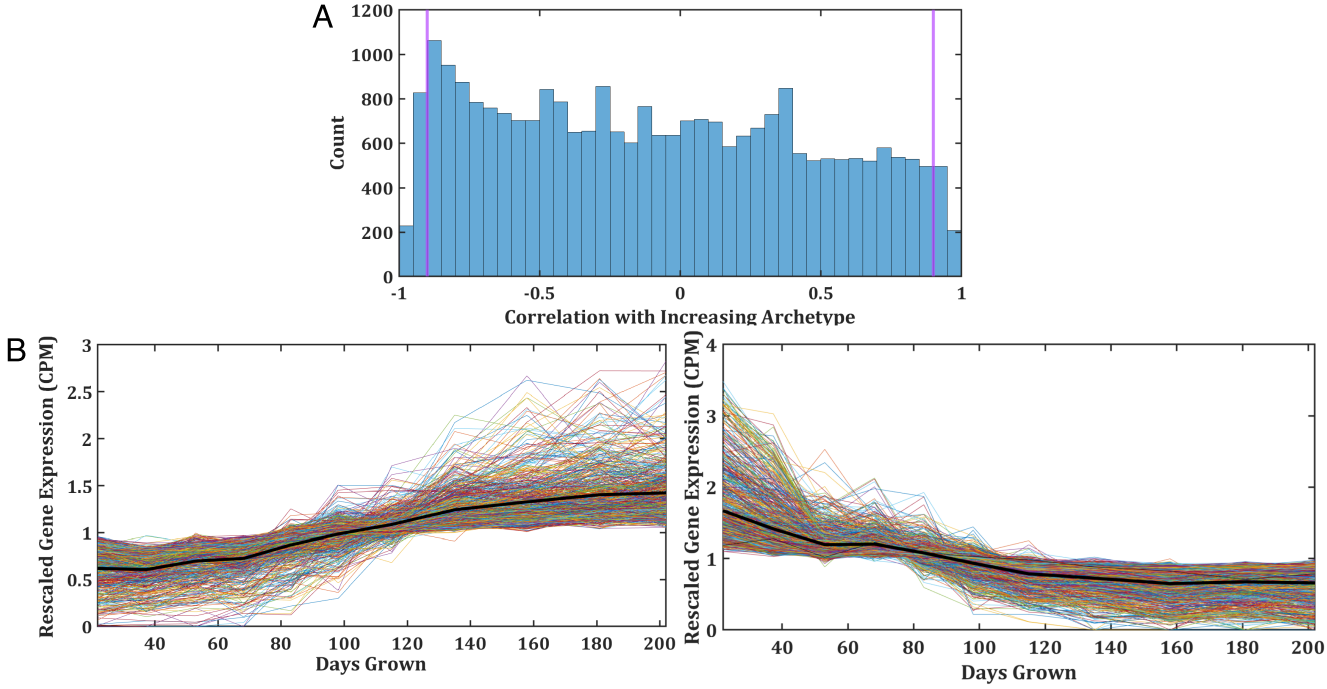

Fig. 5. The transcriptome of human fibroblasts follow similar patterns to *C. elegans* with age. (*A*) Pearson correlation coefficient of all genes vs. the increasing archetypes. Genes with high positive R^2 are strongly monotonically increasing whereas genes with high negative R^2 are monotonically decreasing. Genes selected as archetype centers are to the *Left* and *Right* of the purple lines. (*B*) Rescaled expression data for genes with correlation coefficients ≥ 0.9 (*Top*) and ≤ -0.9 (*Bottom*). Black lines show mean trajectory to better illustrate the shape of the curves.

Discussion

We have distilled the complexity of *C. elegans* aging to an elementary form, showing how a single factor $[f]$ accumulating linearly with age is capable of regulating the concerted drift observed in a large fraction of the aging transcriptome. Both upward and downward gene expression follow Michaelis–Menten or Langmuir-like binding forms, with the activating binding-action of the sensor archetype being less saturated—and thus more linear—than the saturating downward growth archetype.

Previous work by Karin et al. has demonstrated that the linear accumulation of a single factor (namely senescent cells) can explain the Gompertzian survival curves of mice and their temporal scaling behavior (40). Strikingly, the authors also found that this linear accumulation model also applied to organisms such as *C. elegans* where aging is not believed to be driven by senescent cells. Similarly, a stochastic model based on a global state variable captured the Weibull survival curve of *Saccharomyces cerevisiae* (41). Together, these provide additional evidence for the existence of a common key factor within the aging process which could be important at both the transcriptional and organismal level. While the physical identity of this regulating factor $[f]$ remains unknown, there are a few key possibilities.

First, age-related drift in gene expression has been associated with changes in the levels of master regulators such as daf-16 and skn-1(37, 42)—known to control growth and stress resistance (33)—as well as to changes of regulatory miRNAs that impact mRNA turnover (11). While the activity of these regulators (42) may individually not be as smooth as the genome-wide patterns seen here (14), they may collectively shape—and be responsive to—the underlying changes captured by our factor $[f]$.

Second, our factor $[f]$ could reflect the accumulation of a more distributed, bottom–up loss of information. For example, something as basic as making mRNA molecules and their protein products in the correct ratios to form a functional multiprotein complex or pathway fails with age (15, 31, 43–45). This loss of coordination could arise from the accumulation of random changes in the epigenome that impact mRNA production (mRNA-first stoichiometry loss) (14) or may result from less efficient or spatially localized translation and assembly of protein complexes (protein-first stoichiometry loss) (45). Any protein subunits made in excess of the functional ratio would need to be stabilized and degraded, creating a proteostasis burden that scales with the growth rate. Adaptation to this loss of biological coordination would favor the rise of signaling/stress genes and the decline in growth genes seen here.

Last, it should be acknowledged that individual cell types undergo unique aging trajectories at the gene and pathway levels (37). Each cell appears to be adapting to stresses unique to their cell type, activating different sets of stress response genes that delay their aging decline. For example, neurons up-regulate protective skn-1 target genes. At the same time, they strongly down-regulate respiratory metabolism (37), an action that may amplify cell-wide transcriptional changes (46, 47). In contrast, the rise of heat shock proteins is shared across cells, suggesting that protein folding and assembly is a fundamental stress closely related to our factor $[f]$ (37). Moreover, organisms in which cells still reproduce, differentiate, and die during adulthood must age faster than their constituent cells, raising questions about universal eukaryotic programs underlying multiscale aging, which will be interesting to investigate in facultatively multicellular organisms like yeasts (48) and slime molds (49).

In future work, we recommend conducting time course experiments that apply external variations to global variables such as temperature, osmolarity, oxidative stress, and pH, which could potentially give rise to similar changes in the transcriptome as observed in this study (9, 50). By using our archetype analysis methods, it will be possible to distinguish perturbations that accelerate aging, thereby narrowing down the identity of factors involved, and promoting screens for potential antiaging therapies.

Data, Materials, and Software Availability. Previously published data were used for this work NCBI Gene Expression Omnibus (Accession no: GSE63528) (51).

ACKNOWLEDGMENTS. This work was supported by the Laufer Center of Physical and Quantitative Biology at Stony Brook University and by the National Institute of General Medical Sciences Maximizing Investigators' Research Award (MIRA) Program (R35 GM122561). We thank Dr. Michael Petrascheck for his valuable insights and assistance with interpreting the data from Rangaraju et al.

1. T. B. Kirkwood, Understanding the odd science of aging. *Cell* **120**, 437–447 (2005).
2. K. Brys, N. Castelein, F. Matthijssens, J. R. Vanfleteren, B. P. Braeckman, Disruption of insulin signalling preserves bioenergetic competence of mitochondria in ageing *Caenorhabditis elegans*. *BMC Biol.* **8**, 91 (2010).
3. M. E. Harper, S. Monemdjou, J. J. Ramsey, R. Weindruch, Age-related increase in mitochondrial proton leak and decrease in ATP turnover reactions in mouse hepatocytes. *Am. J. Physiol. Endocrinol. Metabol.* **275**, E197–E206 (1998).
4. M. W. Hetzer, The role of the nuclear pore complex in aging of post-mitotic cells. *Aging (Albany NY)* **2**, 74 (2010).
5. Y. Yang *et al.*, Damage dynamics in single *E. coli* and the role of chance in the timing of cell death. bioRxiv [Preprint] (2022). https://doi.org/10.1101/2022.10.17.512406 (Accessed 8 November 2023).
6. I. Liguori *et al.*, Oxidative stress, aging, and diseases. *Clin. Interv. Aging* **13**, 757 (2018).
7. A. Bhattacharya *et al.*, Attenuation of liver insoluble protein carbonyls: Indicator of a longevity determinant? *Aging Cell* **10**, 720–723 (2011).
8. M. Y. Vyssokikh *et al.*, Mild depolarization of the inner mitochondrial membrane is a crucial component of an anti-aging program. *Proc. Natl. Acad. Sci. U. S. A.* **117**, 6491–6501 (2020).
9. M. Santra, K. A. Dill, A. M. de Graff, Proteostasis collapse is a driver of cell aging and death. *Proc. Natl. Acad. Sci. U.S.A.* **116**, 22173–22178 (2019).
10. R. R. Erickson, L. M. Dunning, J. L. Holtzman, The effect of aging on the chaperone concentrations in the hepatic, endoplasmic reticulum of male rats: The possible role of protein misfolding due to the loss of chaperones in the decline in physiological function seen with age. *J. Gerontol. Ser. A Biol. Sci. Med. Sci.* **61**, 435–443 (2006).
11. D. M. Walther *et al.*, Widespread proteome remodeling and aggregation in aging *C. elegans*. *Cell* **161**, 919–932 (2015).
12. P. Liu, R. Song, G. L. Elison, W. Peng, M. Acar, Noise reduction as an emergent property of single-cell aging. *Nat. Commun.* **24**, 680 (2017).
13. C. López-Otín, M. A. Blasco, L. Partridge, M. Serrano, G. Kroemer, The hallmarks of aging. *Cell* **153**, 1194–1217 (2013).
14. S. Rangaraju *et al.*, Suppression of transcriptional drift extends *C. elegans* lifespan by postponing the onset of mortality. *eLife* **4**, e08833 (2015).
15. A. Perez-Gomez, J. N. Buxbaum, M. Petrascheck, The aging transcriptome: Read between the lines. *Curr. Opin. Neurobiol.* **63**, 170–175 (2020).
16. A. S. Anisimova *et al.*, Multifaceted deregulation of gene expression and protein synthesis with age. *Proc. Natl. Acad. Sci. U.S.A.* **117**, 15581–15590 (2020).
17. G. Balázsi, Network reconstruction reveals new links between aging and calorie restriction in yeast. *HFSP J.* **4**, 94–99 (2010).
18. I. Lesur, J. L. Campbell, The transcriptome of prematurely aging yeast cells is similar to that of telomerase-deficient cells. *Mol. Biol. Cell* **15**, 1297–1312 (2004).
19. M. Costa-Mattioli, P. Walter, The integrated stress response: From mechanism to disease. *Science* **368**, eaat5314 (2020).
20. A. Scharf, F. Pohl, B. M. Egan, Z. Kocsisova, K. Kornfeld, Reproductive aging in *Caenorhabditis elegans*: From molecules to ecology. *Front. Cell Dev. Biol.* **9**, 718522 (2021).
21. G. Sturm *et al.*, A multi-omics longitudinal aging dataset in primary human fibroblasts with mitochondrial perturbations. *Sci. Data* **9**, 751 (2022).
22. Y. X. Wang, Y. J. Zhang, Nonnegative matrix factorization: A comprehensive review. *IEEE Trans. Knowl. Data Eng.* **25**, 1336–1353 (2012).
23. D. Barkley *et al.*, Cancer cell states recur across tumor types and form specific interactions with the tumor microenvironment. *Nat. Genet.* **54**, 1192–1201 (2022).
24. C. Weistuch *et al.*, Functional transcriptional signatures for tumor-type-agnostic phenotype prediction. bioRxiv [Preprint] (2023). https://doi.org/10.1101/2023.04.12.536595 (Accessed 10 November 2023).
25. D. D. Truong *et al.*, Mapping the single-cell differentiation landscape of osteosarcoma. bioRxiv [Preprint] (2023). https://doi.org/10.1101/2023.09.13.555156 (Accessed 10 November 2023).

26. Y. Hart *et al*., Inferring biological tasks using pareto analysis of high-dimensional data. *Nat. Methods* **12**, 233–235 (2015).
27. H. Mi, A. Muruganujan, D. Ebert, X. Huang, P. D. Thomas, Panther version 14: More genomes, a new panther go-slim and improvements in enrichment analysis tools. *Nucleic Acids Res.* **47**, D419–D426 (2019).
28. P. D. Thomas *et al*., Panther: Making genome-scale phylogenetics accessible to all. *Prot. Sci.* **31**, 8–22 (2022).
29. P. D. Thomas *et al*., Panther: A library of protein families and subfamilies indexed by function. *Genome Res.* **13**, 2129–2141 (2003).
30. J. Ivanisevic *et al*., Metabolic drift in the aging brain. *Aging (Albany NY)* **8**, 1000 (2016).
31. J. Goldberg *et al*., The mitochondrial ATP synthase is a shared drug target for aging and dementia. *Aging Cell* **17**, e12715 (2018).
32. J. Labbadia, R. I. Morimoto, Proteostasis and longevity: When does aging really begin? *F1000Prime Rep.* **6**, 7 (2014).
33. I. Dhondt *et al*., Foxo/daf-16 activation slows down turnover of the majority of proteins in *C. elegans*. *Cell Rep.* **16**, 3028–3040 (2016).
34. X. X. Lin *et al*., Daf-16/foxo and hlh-30/tfeb function as combinatorial transcription factors to promote stress resistance and longevity. *Nat. Commun.* **9**, 4400 (2018).
35. C. C. Kern *et al*., *C. elegans* ageing is accelerated by a self-destructive reproductive programme. *Nat. Commun.* **14**, 4381 (2023).
36. M. Uno, E. Nishida, Lifespan-regulating genes in *C. elegans*. *NPJ Aging Mech. Dis.* **2**, 1–8 (2016).
37. A. E. Roux *et al*., Individual cell types in *C. elegans* age differently and activate distinct cell-protective responses. *Cell Rep.* **42**, 112902 (2023).
38. G. S. Hotamisligil, R. J. Davis, Cell signaling and stress responses. *Cold Spring Harb. Perspect. Biol.* **8**, a006072 (2016).
39. G. Sturm *et al*., Oxphos defects cause hypermetabolism and reduce lifespan in cells and in patients with mitochondrial diseases. *Commun. Biol.* **6**, 22 (2023).
40. O. Karin, A. Agrawal, Z. Porat, V. Krizhanovsky, U. Alon, Senescent cell turnover slows with age providing an explanation for the Gompertz law. *Nat. Commun.* **10**, 5495 (2019).
41. P. Liu, M. Acar, The generational scalability of single-cell replicative aging. *Sci. Adv.* **4**, eaao4666 (2018).
42. S. T. Li *et al*., Daf-16 stabilizes the aging transcriptome and is activated in mid-aged *Caenorhabditis elegans* to cope with internal stress. *Aging Cell* **18**, e12896 (2019).
43. V. Kogan, I. Molodtsov, L. I. Menshikov, R. J. S. Reis, P. Fedichev, Stability analysis of a model gene network links aging, stress resistance and negligible senescence. *Sci. Rep.* **5**, 13589 (2015).
44. E. Kelmer Sacramento *et al*., Reduced proteasome activity in the aging brain results in ribosome stoichiometry loss and aggregation. *Mol. Syst. Biol.* **16**, e9596 (2020).
45. I. G. Gyuricza *et al*., Genome-wide transcript and protein analysis highlights the role of protein homeostasis in the aging mouse heart. *Genome Res.* **32**, 838–852 (2022).
46. R. P. Das Neves *et al*., Connecting variability in global transcription rate to mitochondrial variability. *PLoS biol.* **8**, e1000560 (2010).
47. R. Guantes, J. Díaz-Colunga, F. J. Iborra, Mitochondria and the non-genetic origins of cell-to-cell variability: More is different. *BioEssays* **38**, 64–76 (2016).
48. J. J. Kuzdzal-Fick, L. Chen, G. Balázsi, Disadvantages and benefits of evolved unicellularity versus multicellularity in budding yeast. *Ecol. Evol.* **9**, 8509–8523 (2019).
49. H. N. Haver, K. M. Scaglione, *Dictyostelium discoideum* as a model for investigating neurodegenerative diseases. *Front. Cell. Neurosci.* **15**, 759532 (2021).
50. N. Stroustrup *et al*., The temporal scaling of *Caenorhabditis elegans* ageing. *Nature* **530**, 103–107 (2016).
51. S. Rangaraju *et al*., "Suppression of Transcriptional Drift Extends C. elegans Lifespan by Postponing the Onset of Mortality". Gene Expression Omnibus. https://www.ncbi.nlm.nih.gov/geo/query/acc.cgi?acc=GSE63528. Accessed 20 June 2022.